

A Chemical Approach for Cell-Specific Targeting of Nanomaterials: Small-Molecule-Initiated Misfolding of Nanoparticle Corona Proteins

Kanlaya Prapainop,[†] Daniel P. Witter,[†] and Paul Wentworth, Jr.*^{†,‡}

[†]Department of Biochemistry, The University of Oxford, South Parks Road, Oxford OX1 3QU, U.K.

[‡]Department of Chemistry and the Skaggs Institute for Chemical Biology, The Scripps Research Institute, 10550 North Torrey Pines Road, La Jolla, California 92037, United States

S Supporting Information

ABSTRACT: A major challenge in nanomaterial science is to develop approaches that ensure that when administered in vivo, nanoparticles can be targeted to their requisite site of action. Herein we report the first approach that allows for cell-specific uptake of nanomaterials by a process involving reprogramming of the behavior of the ubiquitous protein corona of nanomaterials. Specifically, judicious surface modification of quantum dots with a small molecule that induces a protein-misfolding event in a component of the nanoparticle-associated protein corona renders the associated nanomaterials susceptible to cell-specific, receptor-mediated endocytosis. We see this chemical approach as a new and general method for exploiting the inescapable protein corona to target nanomaterials to specific cells.

The past decade has witnessed an explosion in the research on inorganic nanoscale materials for in vivo and in vitro applications as diagnostics and therapeutics. With this research, there is a growing appreciation that the nature of the interactions between components of the biological milieu and the nanoparticle depends upon the structural composition of the xenobiotic and is mediated by surface-bound proteins and lipids, the so-called “protein corona”. Recent work has shown that all nanoparticles in biological fluids are coated with a protein/lipid mélange termed the protein corona.¹ Careful studies have revealed that the composition of this corona is dynamic,² reflects the size, shape, and surface properties of the nanoparticles, and is a major determinant of the localization of the nanomaterials in vivo.³ Therefore, a current challenge in nanomedicine is to develop approaches to ensure that nanoparticles arrive at their site of action in biological systems with their contents intact while at the same time circumventing the effects of the protein corona. The sobering implication of the protein corona is that the in vivo localization of the nanoparticle at the whole-body, organ-system, tissue, cell, and organelle levels ultimately depends not on the nanoparticles’ bulk composition or payload but rather on the identity, organization, and residence time of the proteins at the particle surface. A recent study has shown that negatively charged poly(acrylic acid)-coated gold nanoparticles induce unfolding of bound fibrinogen, promoting the interaction with the integrin receptor MAC-1 and triggering the unwanted inflammatory response common to certain nanomaterials.⁴

In this work, we sought to exploit the nanoparticle/protein corona association in a positive way and use it to target specific cell types in a controlled manner. Thus, we chemically decorated the surface of CdSe/ZnS quantum dots (QDs) with the inflammatory metabolite cholesterol 5,6-secosterol atheronal-B (**1a**) and showed that the resulting nanoparticles (QD585-ath-B, **2a**) bind to and induce the misfolding/aggregation of apolipoprotein B (apo-B₁₀₀) in low density lipoprotein (LDL) and are taken up into cultured macrophages in a cell- and receptor-specific manner (Figure 1).

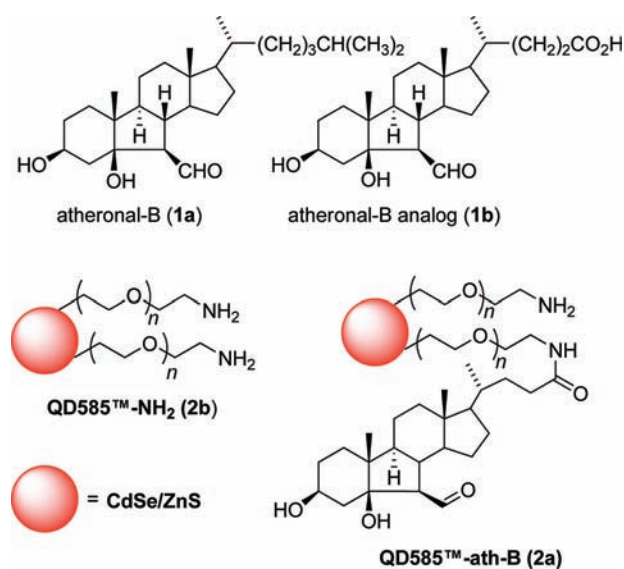


Figure 1. Oxysterols **1a** and **1b** and nanomaterials **2a** and **2b** synthesized for a general approach to cell targeting of nanomaterials.

The core science that underpins our approach to exploit the protein corona stems from our recent discovery of a new class of oxysterol inflammatory metabolites in vivo, termed the atheronals.⁵ What makes the atheronals, such as **1a**, of importance in the context of this study is that we have shown them to perturb the misfolding/aggregation of a number of biologically relevant proteins, such as apo-B₁₀₀,⁵ β -amyloid,⁶ α -synuclein,⁷ antibody light chains,⁸ a murine prion protein⁹ and myelin basic protein. Furthermore, the adduction of **1a** to

Received: January 17, 2012

Published: February 17, 2012

apo-B₁₀₀, the protein component of LDL, causes a conformational change in the protein that exposes epitopes for macrophage cell-surface receptors that ultimately leads to uptake of atheronal-modified LDL particles into cells and foam cell formation.^{5,10}

The nanoparticles selected as a model for this study were fluorescent inorganic CdSe/ZnS QDs possessing an amino-functionalized poly(ethylene glycol) hydrophilic surface, designated as QD585-NH₂ (**2b**). QD585-ath-B (**2a**) was prepared by coupling atheronal-B analogue **1b** (synthesized in three steps from 5-hydroxycholelic acid) to **2b** (~100 amino groups per particle) using EDC and sulfo-NHS in borate buffer as previously described.¹¹ The photophysical properties (absorbance and emission spectra) of **2a** in borate buffer (pH 8.0) were essentially identical to those of **2b** (Figure S1a in the Supporting Information). Fluorescamine analysis revealed that ~50 amino groups remained on each **2a** particle after coupling with **1b**, suggesting that ~50 equiv of **1b** were present on the surface of each nanoparticle. Dynamic light scattering (DLS) confirmed the hydrodynamic radius of **2a** (8.6 ± 0.7 nm) to be slightly greater than that of the starting nanomaterial **2b** (8.0 ± 0.5 nm) and importantly, along with transmission electron microscopy (TEM), also showed that the more hydrophobic nanomaterial **2a** did not measurably aggregate in aqueous buffers when stored for 3 months at 4 °C (Figures S1b–d). The increase in surface hydrophobicity of the atheronal-coated QDs was further confirmed by measurements of the ζ potential, which was considerably less positive for **2a** than **2b** ($\zeta = +2.66 \pm 0.35$ vs $\zeta = +3.51 \pm 0.28$, respectively). A recent shotgun proteomic study by our group established that when incubated in human plasma, QD585-ath-B binds apo-B₁₀₀ and other proteins of the LDL proteome in the so-called “hard corona”.¹¹ In that study, the biological milieu was a cell culture medium, and therefore, the QD585-ath-B nanoparticles were incubated in cell culture medium (RPMI) plus 1% fetal calf serum (FCS), and “hard corona” protein components were resolved on a Tris acetate gel (3–8%) (Figure S2, lane 4). In-gel trypsin digestion and mass spectrometry analysis confirmed that apo-B₁₀₀ (~550 kDa) from bovine LDL in culture medium was indeed bound to nanoparticles **2a**.

To investigate apo-B₁₀₀ misfolding and aggregation, LDL (freshly isolated and purified, TBARS-negative, 40 μ g/mL) was incubated quiescently with oxysterol-functionalized nanoparticles **2a** (200 nM) in aqueous phosphate-buffered saline (PBS, pH 7.4) at 37 °C, and the solution turbidity was measured (Figure 2 inset). In the presence of **2a**, the misfolding and aggregation of apo-B₁₀₀ was accelerated and proceeded with a sigmoidal time dependence, with a lag phase of ~3 h and a time to 50% maximal aggregation (t_{50}) of 6.0 ± 0.2 h (LDL alone has a t_{50} of 32.4 ± 0.4 h under the same conditions). These are indicative of a classical nucleation-dependent polymerization model of aggregation,¹² which typically involves a lag phase where nucleation occurs but turbidity is minimal, followed by a steep rise in turbidity in which amyloid sequence formation is being seeded by the protein nuclei, and finally a plateau phase during which no further amyloid is formed. The way we conceptualize this accelerated aggregation process is as a series of equilibria between apo-B₁₀₀ molecules in LDL and the nanoparticle **2a** (equilibria a–f in Figure 2 are representative examples). Thus, normal apo-B₁₀₀ (represented as two green domains) binds to the oxysterol on **2a** (equilibria a and d) and becomes misfolded (represented as one green and one red domain) (equilibria b and e); the misfolded form may

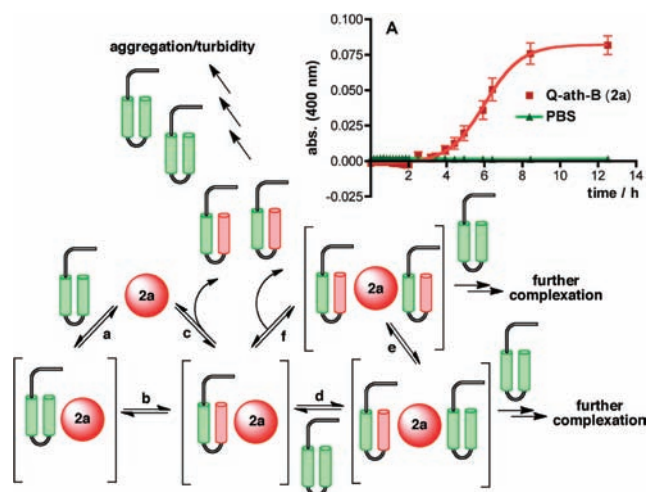


Figure 2. QD585-ath-B (**2a**) nanoparticles induce aggregation of apo-B₁₀₀ in LDL, as represented by the scheme showing several of the plausible equilibria (a–f) established between native apo-B₁₀₀ (two green domains), misfolded apoB₁₀₀ (one green and one red domain), and nanoparticle **2a**. The key equilibria for turbidity are c and f, which release misfolded apo-B₁₀₀ from the nanoparticle into bulk solution. The inset shows the time course of LDL (40 μ g/mL) misfolding, as measured by turbidity (OD at 400 nm), during incubation with **2a** (200 nM) in PBS (pH 7.4) at 37 °C.

either diffuse into the bulk solvent (equilibria c and f) to seed aggregation in solution or stay bound in the corona for either further binding to LDL and/or seeding aggregation on the nanoparticle.

We first studied the uptake of QD585-ath-B (**2a**) into cultured macrophage cells (raw 264.7) using both fluorescence microscopy and flow cytometry (FCM) (Figure 3a,d,g and Figures S3 and S4). In these studies, we used QD585-NH₂ (**2b**) as a control nanomaterial to allow a fair assessment of the effect of surface modification with atheronal **1b**. These initial cell studies revealed concentration- and time-dependent macrophage uptake, with the first QDs appearing in cells after ~30 min and continuing to be taken up even after 4 h of incubation and with measurable uptake of **2a** occurring at 10 nM (Figure 3a,d,g and Figure S4A,B). To confirm that binding of LDL-coated particles alone was not a sufficient trigger for uptake into macrophages, we performed cell-uptake studies with **2b** nanoparticles (100 nM), which also bind LDL in its protein corona (Figure S2, lane 2). This control study showed no macrophage uptake of **2b** (100 nM) after 2 h, whereas under identical conditions **2a** (100 nM) was clearly observed within the cells (Figure S5). Cell viability was not affected by treatment with either **2a** or **2b** in these studies (Figure S6).

A comparison between uptake of **2a** (100 nM) into macrophages incubated for 2 h at 37 °C in RPMI medium supplemented with either FCS (1%, contains lipoproteins), lipoprotein-deficient serum (LPDS, 1%), or delipidated LPDS (1%) revealed a clear requirement of LDL for cell uptake (Figure 3a–c and Figure S7). FCM analysis quantified the difference (measured as the mean fluorescence intensity) as being 2-fold more QDs taken up for the medium supplemented with 1% FCS versus that with 1% LPDS (Figure S7).

Since the above data pointed to an LDL-dependent mechanism of uptake of **2a** into cells, we then studied whether either of the two major receptors responsible for uptake of modified LDL and oxysterols, SR-A and CD36, were

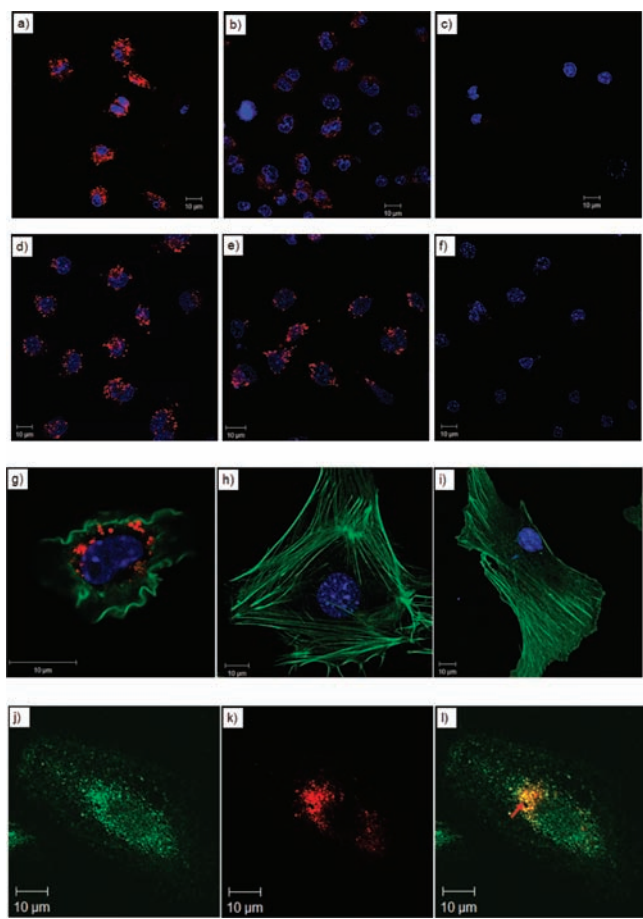


Figure 3. Cell uptake studies of nanomaterial **QD585-ath-B (2a)**. Shown are confocal microscopy images of (unless otherwise stated) raw 264.7 macrophage cells [red, nanoparticle **2a**; blue, 4'-diamidino-2-phenylindole (DAPI); green, phalloidin]. (a–c) Lipoprotein dependence studies. Cells were incubated with **2a** in RPMI medium supplemented with either (a) 1% FCS, (b) 1% LPDS, or (c) 1% delipidated LPDS. (d–f) Receptor dependence studies. Cells were incubated with **2a** pretreated for 30 min with either (d) PBS, (e) anti-SR-A antibody in PBS, or (f) anti-CD36 antibody in PBS. (g–i) Cell-specific uptake studies. Images of the following cells treated with **2a** are shown: (g) murine macrophage (raw 264.7); (h) human dermal fibroblast cells (0038); (i) primary murine glial cells. (j–l) Colocalization studies. Images of a macrophage cell stained with (j) anti-ERp19 antibody (green) and (k) **2a** (red) are shown; (l) is a merge of (j) and (k), with colocalization highlighted by the red arrow (Pearson's coefficient 0.698).

involved.¹³ Thus, we examined whether both antibodies and ligands known to interact with these receptors affected the uptake of **2a**. This study revealed that neither anti-SR-A antibodies nor polyinosinic acid (poly I), which is a known ligand for the SR-A receptor, affected the uptake of **2a** into raw 264.7 cells (Figure 3d,e and Figure S8).¹⁴ In stark contrast, preincubation of cells with an anti-CD36 antibody resulted in significantly reduced uptake of **2a** into cells (Figure 3f).

The scope of this CD36-receptor-mediated uptake of **2a** was explored by studying the uptake of these QDs into cells that do not express either SR-A or CD36 (as validated by FCM; Figure S9). Thus, CD36 null-cultured fibroblast cells and primary astrocyte cells and CD36+ macrophages were incubated with **2a** (100 nM) under identical conditions (RPMI, 1% FCS, 37 °C for 2 h). Fluorescence microscopy confirmed that under

these conditions, **2a** was taken up only into macrophages (Figures 3g–i).

Preliminary trafficking studies of **2a** in cultured macrophages revealed that after 2 h of incubation there was perinuclear localization of **2a** that shared a good degree of colocalization with ERp19 (Pearson's coefficient 0.698), a vesicular marker of the endoplasmic reticulum (ER) (Figure 3j–l and Figure S10). It is known that upon being taken up into cells, LDL travels on the endocytic pathway to late endosomes, after which the lipid components are transferred to the ER for reprocessing and the lipoprotein component to the lysosomes for destruction.¹⁵ While further in-depth trafficking studies are necessary to fully resolve the localization of **2a**, these preliminary data suggest that the ultimate fate of a high percentage of the **QD585-ath-B** in these cells maybe a result of its sterol surface composition.

In conclusion, we have shown that chemical surface modification of nanoparticles with small molecules that can target proteins of the associated corona of the nanoparticles in biological milieu can induce protein misfolding of the associated proteins. This misfolding event can then be used as a trigger for cell-specific uptake of nanomaterials into cells to which they otherwise may not be able to gain access. Given the ubiquitous presence of protein corona on nanomaterials in vivo and the broad interplay between small molecules and protein misfolding, we see this approach as being a potentially wide-ranging approach to the problem of cell-specific targeting of nanomaterials. Looking forward to potential in vivo applications of atheronal-B surface-modified nanomaterials, we envision that the ability either to image or to deliver therapeutic agents selectively to CD36+ cells such as adipocytes, cardiac and skeletal muscle, retinal pigment epithelial cells, and dendritic cells would be a major step forward in nanotechnology.¹⁶ In more general terms, the ability to program the nanoparticle protein corona with small molecules to expose epitopes for a range of receptors could be developed to direct nanoparticles into cell types that they may not have been able to reach before.

■ ASSOCIATED CONTENT

Supporting Information

Methods and supporting figures. This material is available free of charge via the Internet at <http://pubs.acs.org>.

■ AUTHOR INFORMATION

Corresponding Author

paulw@scripps.edu

Notes

The authors declare no competing financial interest.

■ ACKNOWLEDGMENTS

The authors are grateful to Drs. Frederik Karpe and Leanne Hodson (OCDEM) for supplying pure hLDL for this study. Financial support for this work was provided by TSRI, The Skaggs Institute for Chemical Biology, and The Royal Thai Government (predoctoral fellowship for K.P.).

■ REFERENCES

- (1) (a) Colvin, V. L. *Nat. Biotechnol.* **2003**, *21*, 1166–1170. (b) Nel, A.; Xia, T.; Mädler, L.; Li, N. *Science* **2006**, *311*, 622–627. (c) Warheit, D. B.; Webb, T. R.; Sayes, C. M.; Colvin, V. L.; Reed, K. L. *Toxicol. Sci.* **2006**, *91*, 227–236.
- (2) (a) Cedervall, T.; Lynch, I.; Foy, M.; Berggård, T.; Donnelly, S. C.; Cagney, G.; Linse, S.; Dawson, K. A. *Angew. Chem., Int. Ed.* **2007**,

46, 5754–5756. (b) Cedervall, T.; Lynch, I.; Lindman, S.; Berggård, T.; Thulin, E.; Nilsson, H.; Dawson, K. A. *Proc. Natl. Acad. Sci. U.S.A.* **2007**, *104*, 2050–2055.

(3) (a) Lundqvist, M.; Stigler, J.; Elia, G.; Lynch, I.; Cedervall, T.; Dawson, K. A. *Proc. Natl. Acad. Sci. U.S.A.* **2008**, *105*, 14265–14270.

(b) Rocker, C.; Potzl, M.; Zhang, F.; Parak, W. J.; Nienhaus, G. U. *Nat. Nanotechnol.* **2009**, *4*, 577–580.

(4) Deng, Z. J.; Liang, M.; Monteiro, M.; Toth, I.; Minchin, R. F. *Nat. Nanotechnol.* **2011**, *6*, 39–44.

(5) Wentworth, P. Jr.; Nieva, J.; Takeuchi, C.; Galve, R.; Wentworth, A. D.; Dilley, R. B.; DeLaria, G. A.; Saven, A.; Babior, B. M.; Janda, K. D.; Eschenmoser, A.; Lerner, R. A. *Science* **2003**, *302*, 1053–1056.

(6) (a) Zhang, Q.; Powers, E. T.; Nieva, J.; Huff, M. E.; Dendle, M. A.; Bieschke, J.; Glabe, C. G.; Eschenmoser, A.; Wentworth, P. Jr.; Lerner, R. A.; Kelly, J. W. *Proc. Natl. Acad. Sci. U.S.A.* **2004**, *101*, 4752–4757. (b) Scheinost, J. C.; Wang, H.; Boldt, G.; Offer, J.; Wentworth, P. Jr. *Angew. Chem., Int. Ed.* **2008**, *47*, 3919–3922.

(c) Bieschke, J.; Zhang, Q.; Powers, E. T.; Lerner, R. A.; Kelly, J. W. *Biochemistry* **2005**, *44*, 4977–4983.

(7) Bieschke, J.; Zhang, Q.; Bosco, D. A.; Lerner, R. A.; Powers, E. T.; Wentworth, P. Jr.; Kelly, J. W. *Acc. Chem. Res.* **2006**, *39*, 611–619.

(8) Nieva, J.; Shafton, A.; Altobelli, L. J.; Tripuraneni, S.; Rogel, J. K.; Wentworth, A. D.; Lerner, R. A.; Wentworth, P. Jr. *Biochemistry* **2008**, *47*, 7695–7705.

(9) Scheinost, J. C.; Witter, D. P.; Boldt, G. E.; Offer, J.; Wentworth, P. Jr. *Angew. Chem., Int. Ed.* **2009**, *48*, 9469–9472.

(10) Takeuchi, C.; Galve, R.; Nieva, J.; Witter, D. P.; Wentworth, A. D.; Troseth, R. P.; Lerner, R. A.; Wentworth, P. Jr. *Biochemistry* **2006**, *45*, 7162–7170.

(11) Prapainop, K.; Wentworth, P. Jr. *Eur. J. Pharm. Biopharm.* **2011**, *77*, 353–359.

(12) Harper, J. D.; Lansbury, P. T. *Annu. Rev. Biochem.* **1997**, *66*, 385–407.

(13) (a) Kunjathoor, V. V.; Febbraio, M.; Podrez, E. A.; Moore, K. J.; Andersson, L.; Koehn, S.; Rhee, J. S.; Silverstein, R.; Hoff, H. F.; Freeman, M. W. *J. Biol. Chem.* **2002**, *277*, 49982–49988.

(b) Nicholson, A. C.; Han, J.; Febbraio, M.; Silverstein, R. L.; Hajjar, D. P. *Ann. N.Y. Acad. Sci.* **2001**, *947*, 224–228.

(14) van Oosten, M.; van Amersfoort, E. S.; van Berkel, T. J. C.; Kuiper, J. J. *Endotoxin Res.* **2001**, *7*, 381–384.

(15) Chang, T.-Y.; Chang, C. C. Y.; Ohgami, N.; Yamauchi, Y. *Annu. Rev. Cell Dev. Biol.* **2006**, *22*, 129–157.

(16) Febbraio, M.; Silverstein, R. L. *Int. J. Biochem. Cell Biol.* **2007**, *39*, 2012–2030.